Journal of Alloys and Compounds 509 (2011) 9195–9199

Contents lists available at ScienceDirect

Journal of Alloys and Compounds

journal homepage: www.elsevier.com/locate/jallcom

Effects of Sb addition on the modification of Mg_2Si particles and high-temperature mechanical properties of cast Mg–4Zn–2Si alloy

R. Alizadeh, R. Mahmudi*

School of Metallurgical and Materials Engineering, University of Tehran, Tehran, Iran

ARTICLE INFO

Article history:
Received 5 April 2011
Received in revised form 26 June 2011
Accepted 27 June 2011
Available online 2 July 2011

Keywords:
Magnesium alloys
High temperature mechanical properties
Creep
Mg_2Si modification

ABSTRACT

The effect of 2 wt.% Si and 0.2 wt.% Sb on the microstructure and high temperature mechanical properties of a cast Mg–4Zn alloy was investigated. Impression creep, hot hardness, and shear punch tests were used to evaluate the mechanical properties of the alloys at 200 °C. Addition of Si and Sb resulted in the formation of the thermally stable Mg_2Si and Mg_3Sb_2 intermetallic compounds, respectively. By the addition of Sb, the morphology of Mg_2Si particles changed from Chinese script to a more rounded edge type, being capable of providing better plasticity during shear deformation. The presence of thermally stable intermetallic particles and the modified morphology of Mg_2Si particles significantly improved the high temperature mechanical properties of the material.

1. Introduction

Magnesium alloys have been the subject of many research works in recent years. Despite many advantages such as low density, high specific strength and good castability, poor mechanical properties and lack of a stable microstructure at elevated temperatures are the most important barriers on the way of expansion of Mg alloys. Mg–Al alloys are the most common type of magnesium alloys which are used mostly for their moderate strength at room temperature [1–3]. However, they suffer from poor mechanical properties at temperatures above 150 °C, due to the low thermal stability of their main constituent, $Mg_{17}Al_{12}$ compound [3–5]. Therefore, attempts have been made to develop new Mg alloys with sufficient thermal stability at elevated temperatures.

Alloys based on Mg–Zn system are of particular interest for further improvement as new Mg base alloys, because of their pronounced age hardening response. However, due to the appreciable costs usually associated with long solutionizing and aging treatments, it is quite desirable to enhance the high-temperature mechanical properties of Mg alloys in the as-cast condition by the addition of alloying elements such as Si to form high melting point compounds. According to the Mg–Si phase diagram [6], Si has no solubility in solid Mg and its addition results in the formation of the high melting point (1085 °C) Mg_2Si intermetallic compound, which can be beneficial to both creep resistance [7] and high-temperature mechanical properties [8,9]. However, Mg_2Si compound is prone to form as undesirable coarse Chinese script particles under low solidification rates, which are detrimental to mechanical properties. It has also been reported that the presence of the Mg_2Si particles with a Chinese-script morphology in Mg-based composites may not be conducive for providing thermal stability, while it is expected that the massive type of Mg_2Si helps to provide thermal stability, due to its globular shape [10,11]. Therefore, it is of interest to refine the morphology of the coarse Mg_2Si particles.

There have been many attempts to modify the morphology of Mg_2Si particles in the Mg alloys. Ma and co-workers [12,13] reported that the semisolid isothermal heat treatment can modify the Chinese script shaped Mg_2Si phases in the AS91 alloy. They further established that after heat treatment at 560–575 °C for 20 min, the morphology of Mg_2Si phases in the alloy changed from the initial Chinese script shape to granule and/or polygon shapes [12]. In another work [14], tensile strength of a cast Si-containing AZ91 alloy was significantly improved by ultrasonic treatment of the melt. This treatment had a significant effect on the size and distribution of Mg_2Si particles formed during cooling and solidification of the alloy. Surface active elements, such as P, Ca, Ba, Bi, and Sr have been added to Si-containing Mg alloys to modify the morphology of Mg_2Si particles [15–20]. It has also been reported that the modification effect of KBF_4 on the primary and eutectic Mg_2Si in Mg–Si alloy is better than that of K_2TiF_6. This has been attributed to the presence of B in the melts [21]. Recently, it has been shown that, in Mg–Al alloys, modification and refinement of Mg_2Si particles with Sb addition is more effective than that with Ca addition [22]. Improving mechanical properties by combined addition of Si

* Corresponding author. Tel.: +98 21 8208 4137; fax: +98 21 8800 6076.
E-mail address: mahmudi@ut.ac.ir (R. Mahmudi).

0925-8388/$ – see front matter © 2011 Elsevier B.V. All rights reserved.
doi:10.1016/j.jallcom.2011.06.109

and Sb has been confined to the AZ magnesium alloys. It has been shown that addition of Sb to the Si-containing AZ91 alloy results in improved mechanical properties at both room and high temperature [8,23,24]. The aim of this paper is to investigate the effect of 0.2 wt.% Sb addition on the microstructure and high temperature mechanical properties of Mg–4 wt.% Zn–2 wt.% Si alloy, as compared to those of the Mg–4 wt.% Zn base alloy.

2. Experimental procedures

Alloys with nominal compositions of Mg–4Zn, Mg–4Zn–2Si, and Mg–4Zn–2Si–0.2Sb were prepared from high purity (>99.90%) elemental metals. Melting was carried out in a graphite crucible, placed in an electrical resistance furnace under the Foseco Magrex 36 covering flux, to protect magnesium from oxidation. Pouring was accomplished into a steel die preheated up to 150 °C, using a tilt-casting technique, in order to minimize casting defects and the turbulence of the melt. The cast slabs had dimensions of 120 mm × 35 mm × 13 mm, from which 3-mm thick slices were cut using an electrodischarge wire-cut machine for the shear punch test, impression creep, and structural characterization. Scanning electron microscopy (SEM) was used to reveal the microstructural features of the alloys. The energy dispersive spectroscopy (EDS) analysis was performed to reveal the concentration of alloying elements in selected areas of the microstructure. X-ray diffraction analysis was carried out on selected samples to identify the constitutive phases of each alloy.

An MTS universal tensile testing machine equipped with a three-zone split furnace was used to perform impression creep, shear punch, and hot hardness tests in the air atmosphere. The details of testing arrangement of these tests are explained elsewhere [25–27] and will only be briefly described here. In impression creep tests, a flat-ended cylindrical punch 2 mm in diameter was mounted in a holder positioned in the center of the vertical loading bar. The specimen was located on an anvil below the loading bar; the assembly of the specimen and the indenter was accommodated by the split furnace. Measurements were made on each sample at 200 °C and under punch stress of 250 MPa for dwell times up to 4000s. After application of the load, the impression depth was measured automatically as a function of time by the machine; the data were acquired by a computer.

The same configuration was used for the hot hardness tests, in which a cemented-carbide Vickers indenter was mounted in the holder instead of the flat-ended punch. A load of 10 N at an approaching rate of 0.5 mm min^{-1} was applied for a dwell time of 30 s. At least three indentations were made on each sample and the lengths of the diagonals were quantified by an optical microscope. The average values of these diagonals were used to estimate the hardness values. The thin slices of the as-cast materials were ground to a thickness of 0.6 mm, from which disks of 10 mm in diameter were punched for the shear punch test. A shear punch fixture with a 3.175 mm diameter flat cylindrical punch and 3.225 mm diameter receiving hole was used for this experiment. All shear punch tests were performed at 200 °C using a constant cross-head speed of 0.25 mm min^{-1}. The applied load P was measured automatically as a function of punch displacement; the data were acquired by a computer so as to determine the shear stress of the tested materials using the relationship [28]

$$\tau = \frac{P}{\pi dt} \quad (1)$$

where P is the punch load, t is the specimen thickness and d is the average of the punch and die hole diameters.

3. Results and discussion

The XRD patterns shown in Fig. 1 indicate that α-Mg and Mg_4Zn_7 are the only constituents of the base Mg–4Zn alloy. These two phases have also been reported to exist in the as-cast microstructure of the Mg–8Zn [29] alloy. In the Si- and Sb-containing alloys some new peaks corresponding to Mg_2Si and Mg_3Sb_2 intermetallic compounds appear in the patterns, respectively. It is well known that the larger the electronegativity difference between elements, the more is their tendency to form stable compounds. The electronegativity values of Mg, Zn, Si, and Sb are given in Table 1 [30], from which it can be inferred that Si and Sb elements have more tendencies to form a compound with Mg than with each other. Therefore, all of the Sb added to the Si-containing alloy, is consumed to form Mg_3Sb_2 particles and no Si–Sb compound is formed.

The relatively high magnification SEM micrographs of the alloys are shown in Fig. 2. The microstructure of the Mg–4Zn alloy consists of the primary α-Mg matrix and the lamellar eutectic structure, as shown in Fig. 2a. According to EDS analysis, this lamellar eutectic structure shows the composition of $Mg_{42}Zn_{58}$. It is to be noted, however, that due to the very small size of the Mg–Zn particles in the eutectic structure, the quantitative EDS results overestimates the Mg percentage. This can be a result of a large interaction volume of electron beam with the Mg matrix which leads to the emission of X-ray from material beneath the particles. Nevertheless, according to the XRD results these Mg–Zn particles were determined to be Mg_4Zn_7 compound, and thus the lamellar eutectic structure consists of α-Mg + Mg_4Zn_7. As can be seen in Fig. 2b, adding Si to the Mg–4Zn alloy results in the formation of coarse Mg_2Si particles with the undesirable Chinese script morphology, consisting of intersecting major arms and many minor branches having specific orientation relationships. However, as shown in Fig. 2c, addition of only 0.2% Sb to the Si-containing alloy results in the formation of new bright Mg_3Sb_2 particles around the grey Mg_2Si particles and modifies their morphology. In comparison with the Chinese script morphology, the modified particles have rounded edges, with no specific orientation relationship between branches of the particles, and thus, are expected to have a better strain compatibility with the matrix during deformation. EDS analysis indicated that the light particles formed around Mg_2Si particles show the composition of $Mg_{58}Sb_{42}$, which closely corresponds to the Mg_3Sb_2 compound.

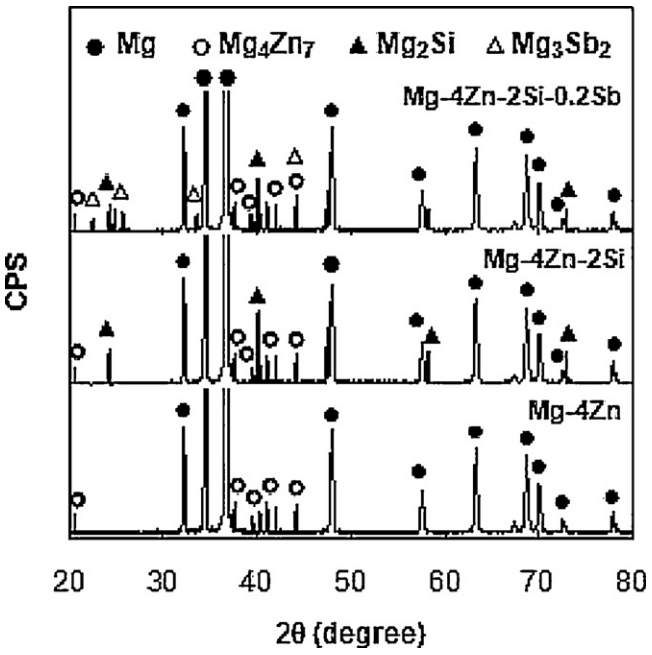

Fig. 1. XRD patterns of the tested alloys.

Yuan and co workers [16] calculated the two dimensional misfit between Mg_3Sb_2 and Mg_2Si particles and showed that when the orientation relationship between these two particles is (0 0 0 1) Mg_3Sb_2//(1 1 1) Mg_2Si, the disregistry is the lowest (5.1%). According to the Bramfitt theory [31], which predicts a limit value of 15% for the two dimensional misfits for heterogeneous nucleation, they suggested that Mg_3Sb_2 could act as the heterogeneous nucleation sites for the Mg_2Si phase by this orientation [16]. It was also proposed that due to the high melting point of Mg_3Sb_2 particles (1245 °C), they should be present before the formation of Mg_2Si particles. However, Mg–Sb has a eutectic alloy system with the

Table 1
Electronegativity of Mg, Zn, Si, and Sb elements [30].

Element	Mg	Zn	Si	Sb
Electronegativity	1.31	1.60	1.80	2.05

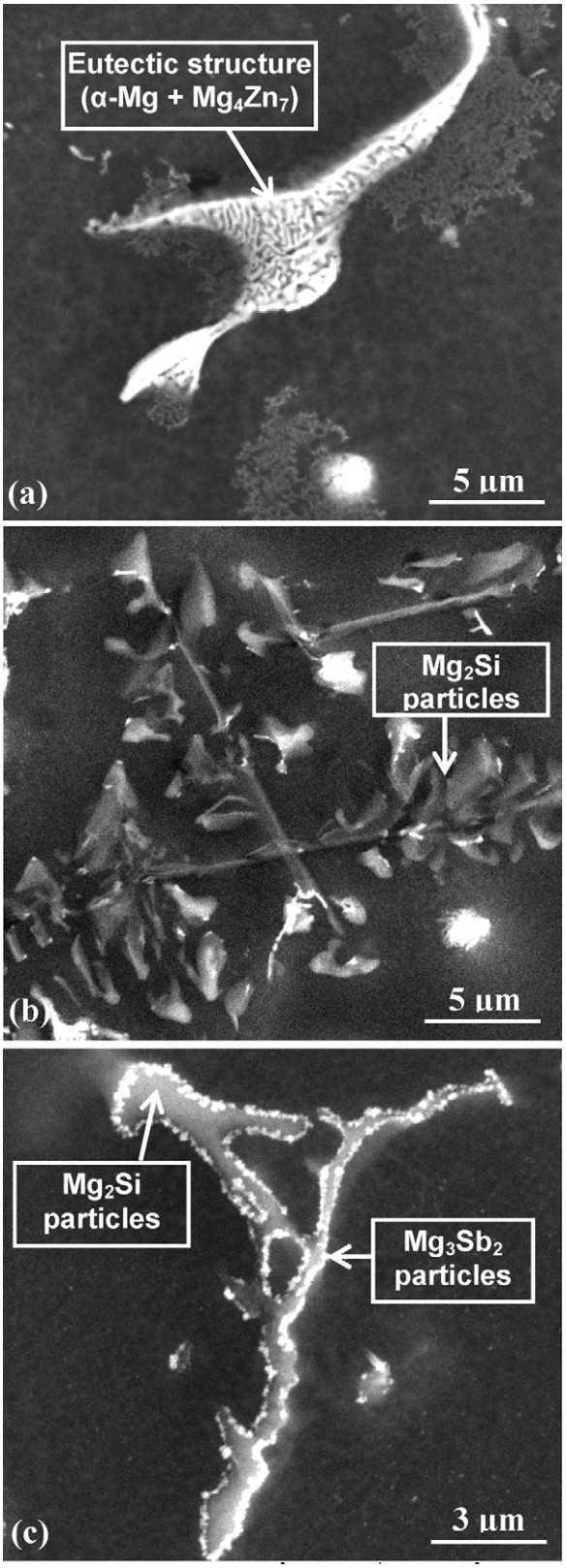

Fig. 2. SEM micrographs showing intermetallic particles in: (a) Mg–4Zn, (b) Mg–4Zn–2Si, and (c) Mg–4Zn–2Si–0.2Sb.

eutectic point of 75 wt. % Sb, and the eutectic temperature of 629 °C [6]. This means that the Mg_3Sb_2 phase precipitates from the Sb-containing magnesium by the eutectic reaction at 629 °C, when the Sb content is less than 75 wt.%. On the other hand, according to the Mg–Si phase diagram [6], the eutectic temperature of this

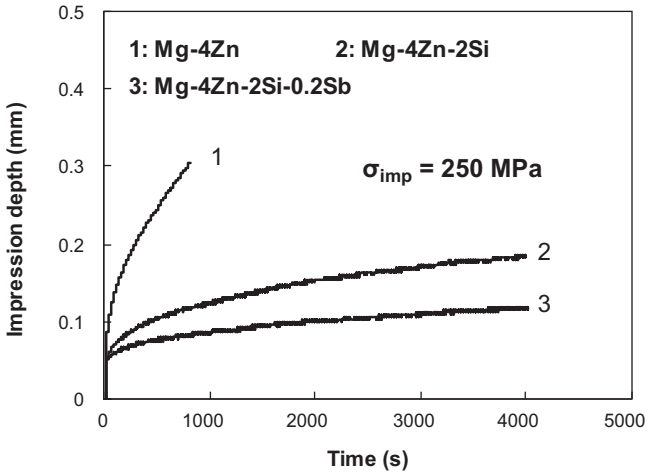

Fig. 3. Impression creep curves of the alloys tested at 200 °C under the punch stress of 250 MPa.

system is 637 °C, which is higher than the precipitation temperature of Mg_3Sb_2 phase. This implies that it is almost impossible for the Mg_3Sb_2 particles to act as heterogeneous nucleation sites for the Mg_2Si phase, as also proposed for Mg–Si–Zn alloys by Zhang et al. [32]. This argument is in agreement with the results obtained in this paper, where it can be inferred from Fig. 2c that the bright Mg_3Sb_2 particles have formed after the formation of the grey Mg_2Si particles and around them.

The observed microstructural features of the studied materials can greatly affect their mechanical properties at elevated temperatures. Results of impression creep tests of the investigated alloys, obtained at 200 °C under the punch stress of 250 MPa, are shown in Fig. 3. As shown in this figure, addition of Si to the Mg–4Zn alloy significantly improves the creep resistance of the base alloy. Similar trends are observed in the shear strength and hot hardness values, shown in Figs. 4 and 5, respectively. This is due to the presence of high melting point Mg_2Si particles with sufficient thermal stability (T_m = 1085 °C [6]), which act as high temperature strengthening particles. Addition of Sb to the Mg–4Zn–2Si alloy further improves the elevated temperature mechanical properties of the alloy, as shown by the lower creep rate, higher shear strength, and higher hot hardness of the Mg–4Zn–2Si–0.2Sb alloy. As mentioned earlier, the achieved enhancement in mechanical properties can be attributed to both formation of thermally stable Mg_3Sb_2 particles and to the morphology modification of Mg_2Si particles. This mor-

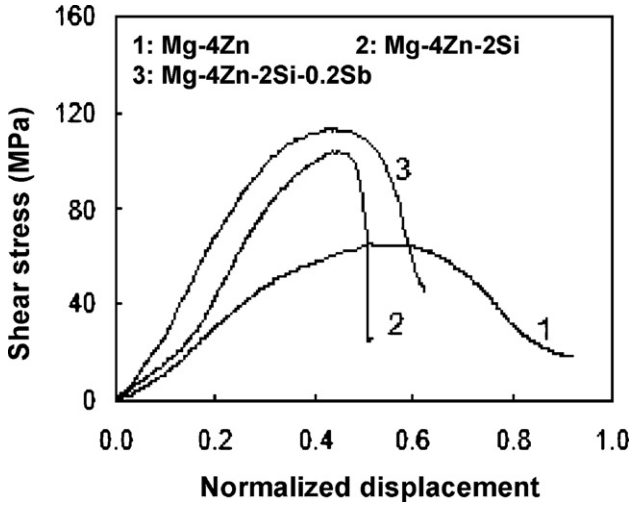

Fig. 4. Shear punch curves of the alloys tested at 200 °C.

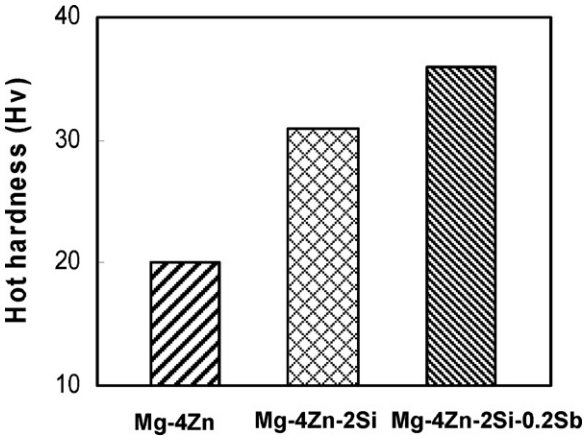

Fig. 5. Hot hardness values of the alloys obtained at 200 °C.

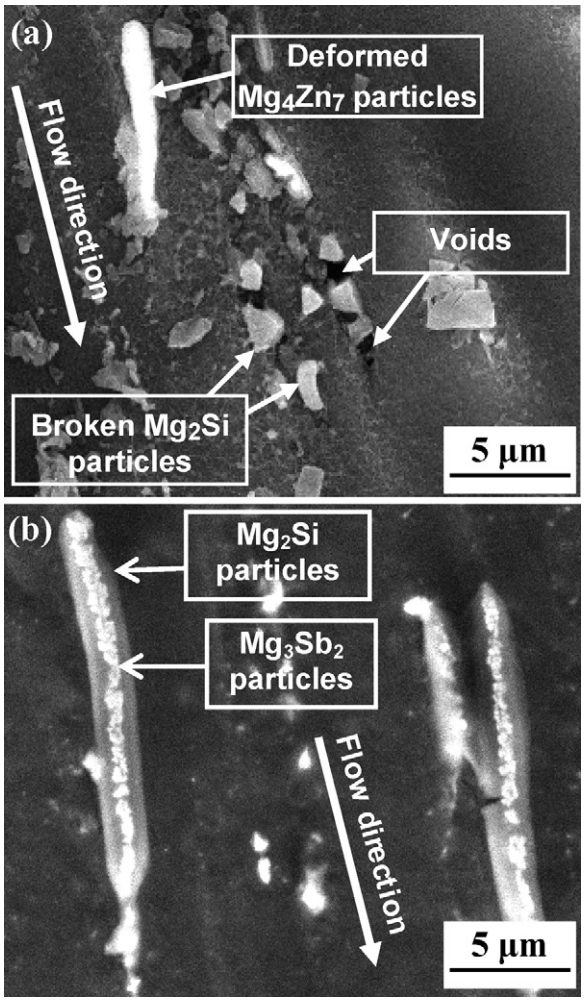

Fig. 6. SEM microstructure of the deformed area under the shear punch for: (a) Mg–4Zn–2Si, and (b) Mg–4Zn–2Si–0.2Sb alloys after SPT at 200 °C.

phology modification also results in an increase of the ductility of the Mg–4Zn–2Si–0.2Sb alloy, as indicated by its higher normalized displacement, compared to that of the Mg–4Zn–2Si alloy, shown in Fig. 4.

In order to study the microstructural evolution of the material during shear deformation, an Mg–4Zn–2Si sample punched at 200 °C was sectioned along the punching direction in the sheared area, as shown in Fig. 6a. It can be seen that while the soft Mg_4Zn_7 particles are deformed and aligned in the flow direction, the harder Mg_2Si particles are broken and dispersed as blocky particles in the Mg matrix. It is also evident that microcracks are formed around some particles, leading to void formation at the interface of the broken Mg_2Si particles and the Mg matrix. This is due to the fact that because of the large stress concentration accumulated on the coarse intersecting branches of Mg_2Si particles, cracks can easily nucleate from the interface between these particles and the Mg matrix, reducing the ductility of the Si-containing alloy. On the other hand, no cracks were found in the microstructure of Mg–4Zn–2Si–0.2Sb under similar conditions, shown in Fig. 6b. In this condition, in contrast to the cast state, the modified Mg_2Si particles are deformed in such a way that they take the shape of jackets encompassing the fine Mg_3Sb_2 particles, the assembly of which being elongated in the flow direction. It is worth noting that there is no evidence of particle breakage or cracks and voids at the particle-matrix interface. This may be ascribed to the better plasticity of the Mg_2Si particles at the investigated test temperature, which can embed the more thermally stable Mg_3Sb_2 particles (T_m = 1245 °C [6]) during large plastic shear deformation. The new microstructural configuration with fine Mg_3Sb_2 particles encapsulated in the modified Mg_2Si phase results in great improvement of mechanical properties of the Mg–4Zn–2Si–0.2Sb alloy.

4. Conclusions

The microstructure of Mg–4Zn consists of the Mg_4Zn_7 intermetallic phase in α-Mg matrix. High temperature mechanical properties of the base alloy was improved by addition of 2 wt.% Si. Further enhancement of these properties was achieved by addition of 0.2 wt.% Sb to the Si-containing alloy. This was accompanied by the formation of Mg_3Sb_2 particles, and modification of the morphology of Mg_2Si particles from coarse Chinese script to finer particles having more rounded edges. The thermally stable Mg_3Sb_2 and Mg_2Si particles, together with the modified morphology of the latter with enhanced plasticity, both improved creep resistance, shear strength and hardness of the material at elevated temperature. Thus, it can be concluded that small addition of Sb to Si-containing Mg–Zn alloys can be beneficial for improving high temperature mechanical properties of the alloy.

Acknowledgment

The authors thank the Iran National Science Foundation (INSF) for providing financial support of this work under Grant No. 89084/87.

References

[1] A.A. Luo, Int. Mater. Rev. 49 (2004) 13–30.
[2] B. Kondori, R. Mahmudi, Metall. Mater. Trans. 40 (2009) 2007–2015.
[3] F. Kabirian, R. Mahmudi, Metall. Mater. Trans. 40 (2009) 116–127.
[4] F. Kabirian, R. Mahmudi, Metall. Mater. Trans. 40 (2009) 2190–2201.
[5] B. Kondori, R. Mahmudi, Mater. Sci. Eng. A 527 (2010) 2014–2021.
[6] ASM Handbook, vol. 3, 1992.
[7] A. Arunachaleswaran, I.M. Pereira, H. Dieringa, Y. Huang, N. Hort, B.K. Dhindaw, K.U. Kainer, Mater. Sci. Eng. A 460–461 (2007) 268–276.
[8] A. Srinivasan, U.T.S. Pillai, B.C. Pai, Metall. Mater. Trans. 36 (2005) 2235–2243.
[9] S.S. Ding, C. Ding, C.Z. Hua, J. Alloy Compd. 470 (2009) L17–L20.
[10] S.K. Thakur, B.K. Dhindaw, N. Hort, K.U. Kainer, Metall. Mater. Trans. 35 (2004) 1167–1176.
[11] Y. Huang, K.U. Kainer, N. Hort, Scr. Mater. 64 (2011) 793–796.
[12] G.R. Ma, X.L. Li, L. Xiao, Q.F. Li, J. Alloy Compd. 496 (2010) 577–581.
[13] G.R. Ma, X.L. Li, L. Li, X. Wang, Q.F. Li, Mater. Charact. 62 (2011) 360–366.
[14] M. Khosro Aghayani, B. Niroumand, J. Alloy Compd. 509 (2011) 114–122.
[15] J.J. Kim, D.H. Kim, K.S. Shin, N.J. Kim, Scr. Mater. 41 (1999) 333–340.
[16] G.Y. Yuan, M.P. Liu, W.J. Ding, I. Akihisa, Mater. Sci. Eng. A 357 (2003) 314–320.
[17] K. Chen, Z.Q. Li, J.S. Liu, J.N. Yang, Y.D. Sun, S.G. Bian, J. Alloy Compd. 487 (2009) 293–297.
[18] J. Hou, C. Li, X. Liu, J. Alloy Compd. 509 (2011) 735–739.

[19] F. Mirshahi, M. Meratian, Mater. Des., in press, doi:10.1016/j.matdes.2011.05.001.
[20] S.G. Lee, J.J. Jeon, K.C. Park, Y.H. Park, I.M. Park, Mater. Chem. Phys. 128 (2011) 208–213.
[21] H.Y. Wang, Q.C. Jiang, B.X. Ma, Y. Wang, J.G. Wang, J.B. Li, J. Alloy Compd. 387 (2005) 105–108.
[22] G.Y. Yuan, Z.L. Liu, Q.D. Wang, W.J. Ding, Mater. Lett. 56 (2002) 53–58.
[23] A. Srinivasan, J. Swaminathan, U.T.S. Pillai, K. Guguloth, B.C. Pai, Mater. Sci. Eng. A 485 (2008) 86–91.
[24] H.Y. Wang, M. Zha, B. Liu, D.M. Wang, Q.C. Jiang, J. Alloy Compd. 480 (2009) L25–L28.
[25] R. Mahmudi, A.R. Geranmayeh, A. Rezaee-Bazzaz, Mater. Sci. Eng. A 448 (2007) 287–293.
[26] R. Alizadeh, R. Mahmudi, Mater. Sci. Eng. A 527 (2010) 3975–3983.
[27] M. Keyvani, R. Mahmudi, G. Nayyeri, Mater. Sci. Eng. A 527 (2010) 7714–7718.
[28] G.L. Hankin, M.B. Toloczko, K.I. Jhonson, M.A. Khaleel, M.L. Hamilton, F.A. Garner, R.W. Davies, R.J. Faulkner, ASTM STP 1366 (2000) 1018–1028.
[29] X. Gao, J.F. Nie, Scr. Mater. 57 (2007) 655–658.
[30] Z.L. Liu, Z.F. Chen, X.Q. Liu, J. Tao, Chin. J. Mater. Res. 20 (2006) 186–190.
[31] B.L. Bramfitt, Metall. Trans. 1 (1970) 1981–1995.
[32] E. Zhang, X. Wei, L. Yang, J. Xu, C. Song, Mater. Sci. Eng. A 527 (2011) 3195–3199.